



Low metals ion source

Vladimir Romanov¹ · Paul Silverstein¹ · Wilhelm Platow¹ · Justin McCabe¹ · Olivia Campbell¹ · Kevin Wenzel¹ · Ronald Reece¹

Received: 16 September 2024 / Accepted: 6 March 2025
© The Author(s), under exclusive licence to The Materials Research Society 2025

Abstract

Energetic metal contamination is a significant contributor to white pixel defects and high dark current in CIS devices (Teranishi in *Sensors* 18:2358, 2018). Multiply charged Fe, Ti, Cr, Cd, W, Mo, and V ions can have similar magnetic and electrostatic rigidity as high-energy implant species, such as As²⁺, As³⁺, and As⁴⁺ and therefore are insufficiently removed by magnetic or electrostatic filtering. This paper discusses in detail the source of these impurities and steps taken to minimize the contamination as part of the development of the Axcelis' ELS Low Metals ion source upgrade kit.

Introduction

Low-level metallic contaminants are becoming a more prevalent device risk causing high white pixel counts and dark current within CMOS image sensor (CIS) devices as well as diminished carrier lifetimes, dielectric breakdown of gate oxides, threshold voltage shifts, and increased junction leakage currents [1]. Manufacturing and future development of leading edge CMOS (complementary metal oxide semiconductor) image sensors require high-energy arsenic ion implants up to 8 MeV. To reach these energies, ions of a higher charge state (up to 4+) are extracted from the ion source. The Purion VXE platform for example can reach 8-MeV energies utilizing quadruply charged phosphorus and arsenic ions.

The drawback of using As⁴⁺ ions for achieving high energies is the magnetic rigidity overlap with ⁵⁶Fe³⁺ present in the beam. Traces of iron will be able to pass through the mass analyzer together with As⁴⁺ due to the small $\Delta m/z$ of 0.08 [2]. To produce high charge state ions requires running the ion source close to maximum power. This will increase the sputter rate of arc chamber walls which can lead to an increase in iron plasma concentrations [3]. It is standard practice in the semiconductor industry to use high-purity refractory metals, such as tantalum or tungsten in the design of the ion sources. Nevertheless, trace amounts of iron are

still present in the bulk of the material at the ppm level and can be transferred to the gas phase through sputtering. The use of high arc power will also raise the temperature of the arc chamber and its surroundings. High surface temperatures will result in increased rates of chemical etching and sublimation of the non-refractory parts outside of the arc chamber. The question arises which of these three mechanisms is the major source for iron transport into the plasma.

This paper describes a partitioning approach to determine the primary mechanism of iron transport into the ion beam and subsequently determines the major contributors for the iron contamination in the arc chamber and its surroundings.

Materials and methods

All implantations were performed on an Axcelis Purion XE-series high-energy implanter. The implanted doses were from 5×10^{13} at/cm² to 1×10^{16} at/cm² to provide reliable SIMS (Secondary Ion Mass Spectrometry, Cameca) measurements with low background noise and minimal damage accumulation effects on dopant profiles. SIMS analysis was performed on one-inch Ge wafers implanted with MeV range energies using multiply charged ⁷⁵As ions. Bulk Silicon Etch (BSE) Inductively Coupled Plasma Mass Spectrometry (ICP-MS, PerkinElmer) trace level metals contamination analysis was conducted using 300-mm Si wafers implanted within the same energy and dose range. Glow Discharge Mass Spectrometry (GDMS, Nu Instruments) was used to determine quantitative elemental compositions of arc chamber components and adjacent hardware. An ion source test

✉ Vladimir Romanov
vladimir.romanov@axcelis.com

¹ Axcelis Technologies, 108 Cherry Hill Drive, Beverly, Massachusetts 01915, USA

stand was utilized to record the temperature of ten test points around the arc chamber at various power settings (700 W to 1500 W, Fig. 1a and b). Temperature readings were taken at steady-state conditions. The total power was calculated based on the filament, cathode, and arc power settings.

Results and discussion

Design methodology

The material-dependent contribution of ion source parts to metal extraction was limited to sublimation, sputtering, and chemical etching. High sputtering rates are expected within the arc chamber. We can therefore estimate the transfer of impurities such as iron by sputtering of tungsten parts in the arc chamber. We can expect a single digit ppm level of Fe^{3+} in the quadruply charged arsenic implant, which is also the typical level of iron in the tungsten parts. For this calculation, we assumed the following: 1% efficiency of ionization for As and Fe; negligible diffusion of iron in tungsten, a sputter rate of W/Fe by arsenic ions of around 10% [4]; and

ion current fractions for $\text{As}^{4+}/\text{As}^+$ and $\text{Fe}^{3+}/\text{Fe}^+$ of 0.1% and 1%, respectively [5]. Sputtering of tungsten in the arc chamber by itself cannot explain previously reported levels of iron contamination in the As^{4+} implant [2].

For metal impurities generated by sublimation, we identified areas of high temperature outside the arc chamber (Fig. 1a and b) and evaluated the vapor pressure of the exposed materials (Fig. 1c) [4]. Ten thermocouples were used to get complete coverage of temperature of the arc chamber and its surrounding during ion implantation over a wide range of arc power. The highest temperature (1100 °C) was recorded by a thermocouple (TC1) installed between the liner and the internal wall of the arc chamber at maximum power of the ion source. A second hot zone of 960 °C (TC7) was found at the cathode side. The arc slit and the external walls of the arc chamber (TC5, TC6, and TC10) reached a temperature of 820 °C. Lower temperatures were found at the base of the arc chamber, the gas line, and repeller and were within 630 to 740 °C.

Based on the temperature of the base of the arc chamber, we can roughly calculate the transfer of iron by sublimation from the gas line to the arc chamber. The pressure inside

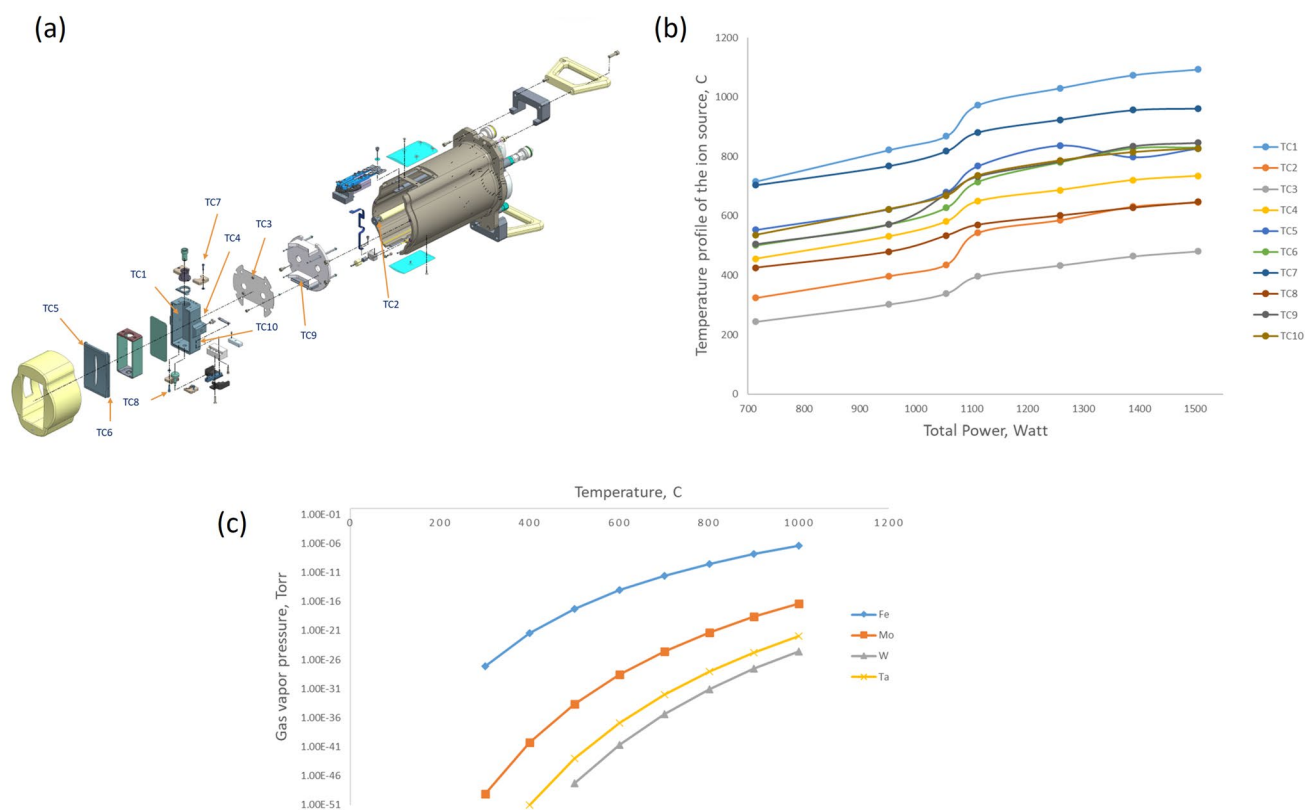
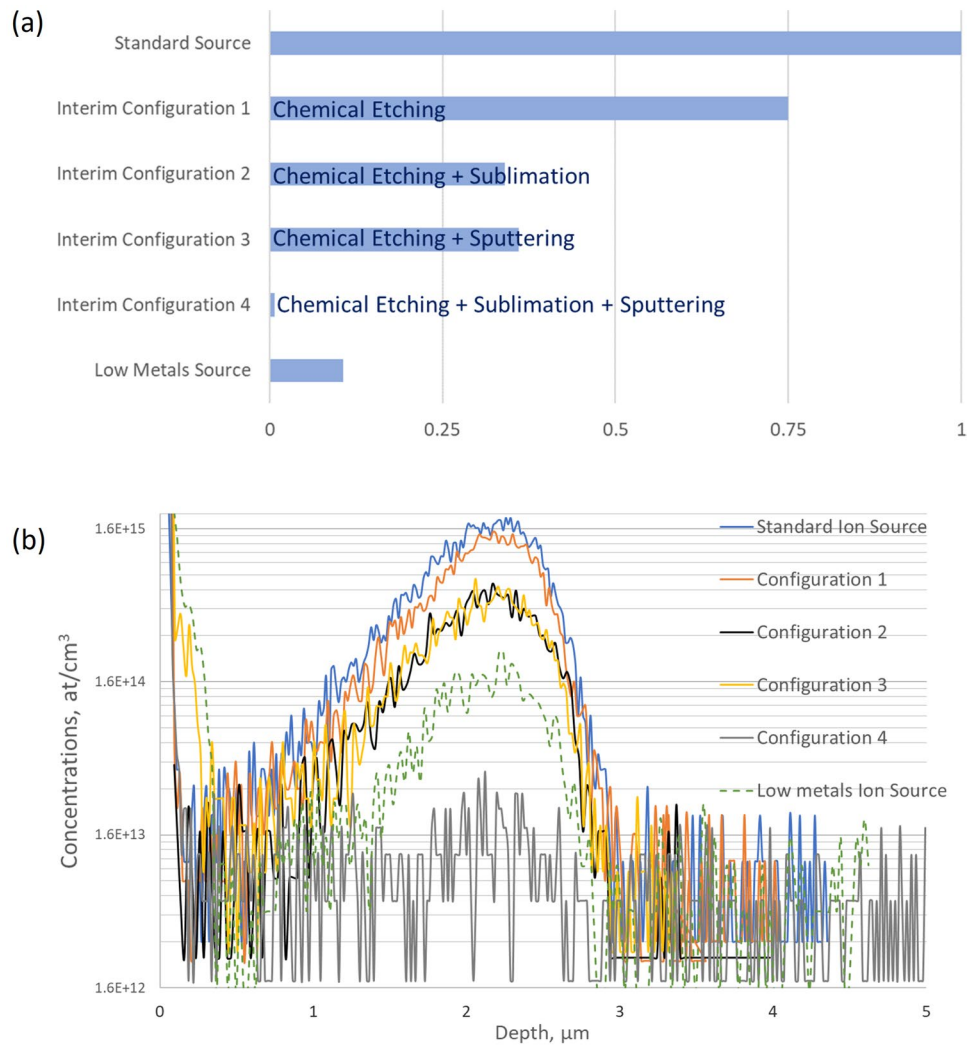


Fig. 1 Ten thermocouples were installed on the Purion ion source **a** and data points collected as a function of ion source power **b**: TC1—Source liner; TC2—Gas line at the bottom of arc chamber; TC3—Heat shield; TC4—Bottom of the arc chamber; TC5—Arc slit at the

cathode side; TC6—Arc slit at the repeller side; TC7—Insulator at the cathode side; TC8—Insulator at the repeller side; TC9—Stand-offs; and TC10—Side of the arc chamber. Modeled vapor pressures of Fe, Mo, W, and Ta as a function of temperature **c** [4]

Fig. 2 **a** Stepwise reduction of ^{56}Fe contamination using partitioning approach. Normalized ^{56}Fe concentration in As^{4+} 6.0-MeV 5×10^{14} at/cm 2 implant. **b** SIMS depth profiles of ^{56}Fe in an As^{4+} 5×10^{14} at/cm 2 6-MeV implant



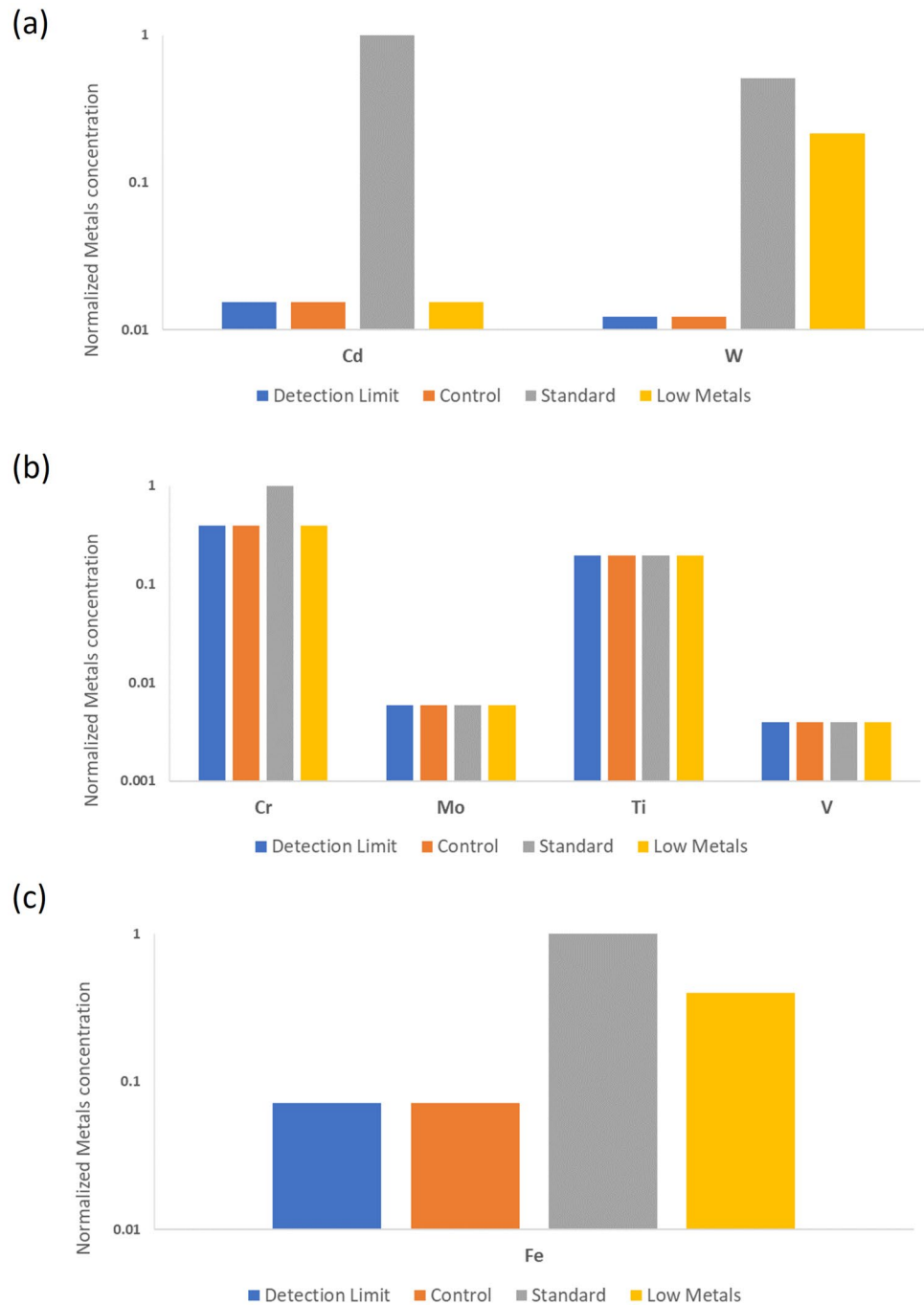
the arc chamber is typically 1×10^{-3} Torr (AsH_3). The vapor pressure of Fe is 2.2×10^{-11} Torr at a temperature of 740°C as measured for the gas line and the base of the arc chamber. The iron contamination therefore will be in ppb range. However, if stainless steel hardware is used on the cathode side of the arc chamber, it can act as a secondary iron contamination source since the vapor pressure of Fe is considerably higher (1.1×10^{-7} Torr) at a local temperature of 960°C . Stainless steel (SS) and molybdenum (Mo) should be avoided as a material for ion source parts which experience high temperatures in vacuum; for SS parts, a conservative limit is 400°C and for Mo 800°C (Fig. 1c). A suitable alternative would be refractory metals such as tungsten or tantalum due to their low vapor pressure at maximum arc power.

Similarly, materials in areas susceptible to chemical etching were identified. Estimation of the magnitude of iron

contamination in arsenic implants through chemical etching is a challenge due to the various materials used and the lack of rate constants. Instead, materials were grouped within each of the three extraction mechanisms and then subjected to SIMS analysis.

For the sublimation mechanism, regions of high temperature outside the arc chamber were identified and higher-purity or alternative materials were tested. For the sputtering mechanism, the search for the source of the trace contaminant was limited to the arc chamber. Higher-purity or alternative materials were tested. Finally, for chemical etching, materials sensitive to etching at higher temperatures were determined and replaced by chemically inert or higher-purity materials. In all cases, SIMS analysis was used to evaluate the reduction of energetic $^{56}\text{Fe}^{3+}$ contamination level in $^{75}\text{As}^{4+}$ implant.

Fig. 3 Bulk concentration of metal contamination (2- μm BSE ICP-MS): **a** Normalized Cd and W concentration in doubly charged arsenic implant (dose 1×10^{16} at/cm 2 at 1700 keV). **b** Normalized Cr, Mo, Ti, and V concentration in triply charged arsenic implant (dose 1×10^{15} at/cm 2 at 2000 keV). **c** Normalized Fe concentration for quadruply charged arsenic implants (dose 5×10^{13} at/cm 2 at 2000 keV)



Partitioning experiment

We measured $^{56}\text{Fe}^{3+}$ for energetic metals contamination in As^{4+} implants (6.0 MeV , 5×10^{14} at/cm 3 , 25 mm germanium wafer), employing SIMS to evaluate improvement and BSE ICP-MS for validation. Typical detection limits for ^{56}Fe are 2×10^{12} at/cm 3 in Ge wafers and 5×10^{15} at/cm 3 in Si wafers [6] due to the mass interference between $^{56}\text{Fe}^+$ and $^{28}\text{Si}_2^+$ [7].

Figure 2b shows the results of stepwise reduction of ^{56}Fe contamination using a partitioning experiment. We were able to achieve 25% reduction of iron contamination by replacing parts that were susceptible to chemical etching (Fig. 2a and b, interim configuration 1). In configuration 2, we replaced external components with a material (tungsten) that has a lower sublimation rate at a given temperature of the ion source, which in return reduced energetic contamination by

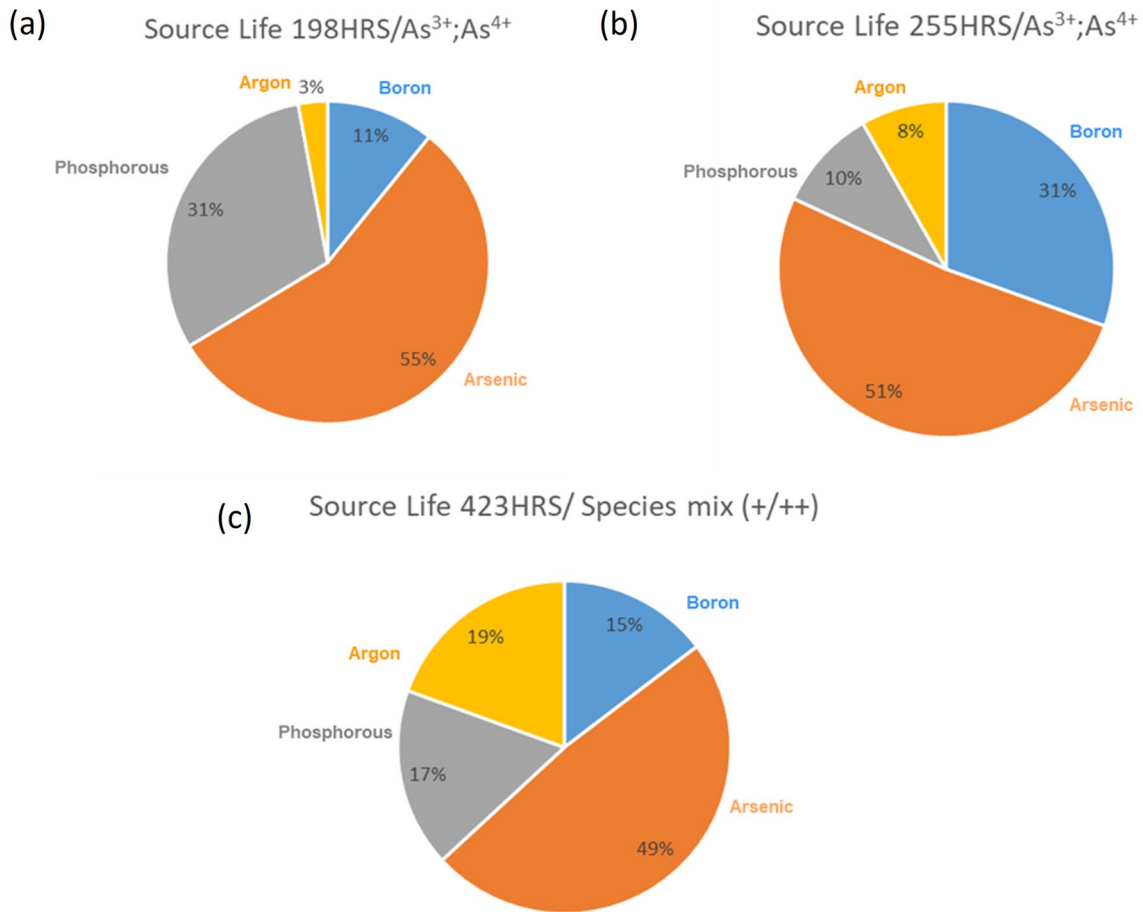


Fig. 4 Lifetime tests of upgrade kit: **a** 198 h of multi-charge arsenic and phosphorous implants; **b** 255 h of multi-charge arsenic and boron implants; and **c** 423 h of singly and doubly charged arsenic, phosphorous, and boron implants

an additional 41%. Interim configuration 3 has all the components from configuration 1 and, in addition, all the internal parts of the arc chamber were replaced with ultra-pure material (low ppm level of metals contamination) resulting in 39% reduction of iron. The iron peak at $2.13 \mu\text{m}$ was almost eliminated for interim configuration 4 (all the components from configuration 2 and 3). The ^{56}Fe reduction trend chemical etching < sputtering < sublimation was found. Based on the data available, we were able to optimize critical internal and external parts to produce a cost-effective low metal source upgrade kit with 90% reduction of energetic iron contamination (Fig. 2a, b).

Low metals ion source upgrade kit

BSE ICP-MS trace level metals contamination analysis was conducted using 300-mm Si wafers implanted within the same energy and dose range. Using Surface Metal Vapor Phase Decomposition (VPD) ICP-MS, we analyzed each

wafer prior to the BSE ICP-MS analysis. Based on bare Si wafers, control wafers measured at or below detection limit. Figure 3a shows a reduction of $^{112}\text{Cd}^{3+}$ in doubly charged arsenic implant (dose 1×10^{16} at/cm² at 1700 keV) for the low metal upgrade kit. Since tungsten is the main material used in the construction of the arc chamber, apparent W improvement is not significant. Furthermore, Mo, Ti, and V are below detection limit for both configurations of the ion source apart from Cr (Fig. 3b) in triply charged arsenic implants (dose 1×10^{15} at/cm² at 2000 keV). Also shown is a threefold Fe reduction (Fig. 3c) in quadruply charged arsenic implant (dose 5×10^{13} at/cm² at 2000 keV) which is in good qualitative agreement with the SIMS results.

All the changes to the ion source hardware did not affect lifetime in comparison with the standard hardware (Fig. 4a–c). We achieved 198 h for multi-charged arsenic and phosphorus implants; 255 h for multi-charged arsenic and boron implants; and 423 h for singly and doubly charged arsenic, phosphorus, and boron implants.

Conclusion

The primary mechanism of iron transport into the ion beam and major contributors of iron in the arc chamber and its surroundings were determined. Major source of energetic iron contamination was sublimation of the non-refractory parts in close proximity to the arc chamber. Subsequently, this information was used to replace critical internal and external parts yielding a cost-effective low metal source upgrade kit with a 90% reduction of energetic iron contamination without compromising performance and lifetime. The Low Metals Ion Source coupled with the industry leading metals filtration of the Purion VXE beamline provides the lowest metals contamination for customers who need best-in-class beam purity.

Acknowledgments The authors would like to thank Eurofins EAG Laboratories for the SIMS analysis of high energy-implanted dopant profiles in the 25-mm germanium wafers and GDMS analysis of arc chamber and adjacent components and Chemtrace for the BSE-ICP-MS analysis of the 300-mm silicon wafers.

Author contributions All authors contributed to the study, conception, and design. Material preparation, data collection, and analysis were performed by Vladimir Romanov. The first draft of the manuscript was written by Vladimir Romanov and all authors commented on previous versions of the manuscript. All authors read and approved the final manuscript.

Funding No funds, grants, or other support were received.

Data availability The datasets generated during and/or analyzed during the current study are available from the corresponding author on reasonable request.

Declarations

Competing interests The authors have no competing interests to declare that are relevant to the content of this article.

References

1. N. Teranishi, G. Fuse, M. Sugitani, A Review of ion implantation technology for image sensors. *Sensors (Basel)*. **18**(7), 2358 (2018)
2. S. Satoh, W. Platow, S. Kondratenko et al., Purion XEmax, axcelis ultra-high energy implanter with Boost™ technology. *MRS Advances* **7**, 1490–1494 (2022)
3. H. Ryssel, R. Heiner, M. Current, L. Frey, *Contamination control for ion implantation, ion implantation, science and technology* (1996)
4. Vapor Pressure Calculator [IAP/TU Wien]
5. S. Satoh, Acceleration of 4+ions in an RF linac accelerator, 2018 22nd international conference on ion implantation technology (IIT), (Würzburg, Germany, 2018), pp. 295–298
6. M-033218-Secondary-Ion-Mass-Spectrometry-Survey-Depth-profile.pdf (eag.com)
7. R.A. De Souza, M. Martin, Secondary ion mass spectrometry (SIMS)—a powerful tool for studying mass transport over various length scales. *Phys. Status Solidi (c)* **4**, 1785–1801 (2007)

Publisher's Note Springer Nature remains neutral with regard to jurisdictional claims in published maps and institutional affiliations.

Springer Nature or its licensor (e.g. a society or other partner) holds exclusive rights to this article under a publishing agreement with the author(s) or other rightsholder(s); author self-archiving of the accepted manuscript version of this article is solely governed by the terms of such publishing agreement and applicable law.